Examining the impact of multiple climate forcings on simulated Southern Hemisphere climate variability

Asmerom F. Beraki [1,2,*], Yushi Morioka[4], Francois A. Engelbrecht[3], Masami Nonaka[4], Marcus Thatcher5, Nomkwezane Kobo[1] and Swadhin Behera[4]

[1] CSIR-Smart Places, Holistic Climate Change Impact, Pretoria, South Africa
[2] Department of Geography, Geoinformatics and Meteorology, University of Pretoria, Pretoria, South Africa
[3] Global Change Institute, University of the Witwatersrand, Johannesburg, South Africa
[4] Application Laboratory, JAMSTEC, Yokohama, Japan
[5] CSIRO Marine and Atmospheric Research, Aspendale, Victoria, Australia

* Correspondence to: Asmerom F. Beraki. Email: asmiefb@gmail.com

Abstract

The study examines the influence of external climate forcings, and atmosphere–ocean–sea–ice coupled interaction on the Southern Hemisphere (SH) atmospheric circulation variability. We analysed observed and simulated changes in view of Antarctic sea–ice and Southern Ocean surface temperature trends over recent decades. The experiment embraces both idealised and comprehensive methods that involves an Earth System Model (ESM) prototype. The sensitivity experiment is conducted in a manner that decomposes the signatures of sea–ice, sea surface temperature and feedback mechanisms. The results reveal that the Southern Annular Mode (SAM) multidecadal variability is found to be modulated by coupled interactions whereas its sub-seasonal to interannual vacillation seems to follow a random trajectory. The latter may strengthen the notion that its predictability is limited even with the use of ESMs. Most of the atmospheric circulation variability and recent changes may be explained by the ocean thermal forcing and coupled interactions. However, the influence of sea–ice forcing alone is largely indistinguishable and predominantly localised in nature. The result also confirms that the Antarctic dipole-like sea–ice pattern, a leading climate mode in the SH, has intensified in the last three decades irrespective of season. The probable indication is that processes within the Southern Ocean may play a key role, which deserves further investigation.

Keywords: Dipole-like sea–ice pattern; Coupled interaction; Feedback mechanism; ESM; Model sensitivity; SAM

Introduction

Southern Hemisphere (SH) climate variability is characterised by the variations in quasi-stationary and zonally propagating waves in the atmospheric circulation (Wallace and Hsu 1983; Berbery et al. 1992; Ambrizzi et al. 1995). The leading modes of climate variability and possible mechanisms responsible for their maintenance have recently been reported on by a number of studies (e.g., Colberg et al. 2004; White and Simmonds 2006; Morioka et al. 2013; Wang and Dommenget 2016). Within this context, the connection of tropical forcing to extra-tropical and polar climate regimes has become a particular area of focus (e.g., Li et al.

2014; Turney et al. 2017). This line of investigation has seemingly been motivated, to some extent, by the fact that trends in Antarctic sea–ice concentrations are not simply mirroring the systematic decline of the Arctic sea–ice (Yuan and Martinson 2001; Holland and Kwok 2012; Li et al. 2014; Hobbs et al. 2016). In addition, the response of the Southern Ocean to an increase in the concentration of greenhouse gases in the atmosphere is delayed or dampened, presumably due to its large heat capacity (Stouffer et al. 1989; Bi et al. 2001; Goosse and Renssen 2001). One complication in studying the trends and variability in Antarctic sea–ice is that most climate models including those participated in the Coupled Model Intercomparison Project Phase Five (CMIP5) have noticeable deficiencies in simulating its redistribution and changes (e.g., Hosking et al. 2013; Mahlstein et al. 2013; Purich et al. 2016).

The response of Antarctic sea–ice to atmospheric forcing is spatially heterogeneous and is argued to incorporate complex feedbacks among the atmosphere, sea–ice, and ocean. The contrasting sea–ice trends of the Amundsen, Bellingshausen, and Ross Seas are suggested to be associated with the deepening of the Amundsen Sea Low (ASL) in recent decades (Turney et al. 2016), tropical forcing (Yuan and Martinson 2001; Ding et al. 2011; Schneider et al. 2012; Jones et al. 2016), radiative forcing (Fogt and Wovrosh 2015) and the phase of the southern annular mode (SAM, Hall and Visbeck 2002; Lefebvre et al. 2004; Simpkins et al. 2012). However, several studies have attributed observed trends to local forcings including, inter alia, varying influences of the surface wind (Holland and Kwok 2012), dynamic and thermodynamic processes in the ice pack (Holland et al. 2005), the interaction with the Southern Ocean (Swart and Fyfe 2013), and the modification of the hydrological cycle (Liu and Curry 2010). In addition, sea–ice variability and large-scale atmospheric circulation mechanisms which include, among others, the zonal wave 3 (ZW3, Raphael 2007), the semi-annual oscillation (Van Den Broeke 2000), the El Niño–Southern Oscillation (ENSO, Turner 2004; Yuan 2004), ozone depletion (Fogt and Zbacnik 2014), and the Atlantic Multidecadal Oscillation (AMO, Li et al. 2014) may manifest distinct causality at different temporal scales.

Although the drivers and feedbacks of Antarctic sea–ice trends and variability remain highly uncertain, the prime mechanism by which tropical forcing drives Antarctic atmospheric circulation critically dependent on poleward propagating Rossby wave trains (Ding et al. 2011) where the Antarctic Circumpolar Current (ACC) acts as a conduit to tropical forcing (Yuan and Martinson 2001). In the Pacific sector, the same physical process is found to be instrumental in transporting equatorial Pacific temperatures across mid- to high-latitudes during austral spring and summer (Turney et al. 2017). Wave trains are embedded within the Pacific–South America (PSA) mode of climate variability (Karoly 1989; Mo and Higgins 1998; Ding et al. 2011; Trenberth et al. 2014). In the Atlantic sector, however, their role is restricted to the austral winter, with only a marginal teleconnection with the Amundsen Sea during summer because the Rossby wave trains are trapped in the subtropics (Li et al. 2014).

The role of sea–ice forcing on atmospheric and oceanic circulation, and its relative contribution to climate interactions is potentially of importance in mid- and high-latitude climate predictability (Lemke et al. 1980; Raphael 2003; Goosse and Zunz 2014; Hobbs et al. 2016; Jones et al. 2016; Morioka et al. 2017). Previous studies (e.g., Mitchell and Senior 1989; Simmonds and Wu 1993) have examined the impact of Antarctic sea–ice distribution on SH atmospheric circulation focusing primarily on the austral winter ocean/atmosphere turbulent heat response. These studies showed that the reduction in sea–ice concentration (SIC) may result in induced atmospheric warming associated with changes in the sensible heat flux which may result in westerly (easterly) wind anomalies occurring south of 60° S (between 45° and 60° S) with an increase in the number of cyclones close to Antarctica and a

decrease in this number further north. Based on two case studies from atmospheric model simulations forced with prescribed sea surface temperatures (SSTs), Hudson and Hewitson (2001) suggested that local changes in sea–ice extent had impacts on circulation remote from the region of change during austral summer. Raphael (2003) used an ocean–atmosphere coupled climate model prescribed with SIC extremes to examine the impact of sea–ice forcing on atmospheric circulation during the same season and concluded that SIC forcing triggered local thermal and nonlocal dynamic responses in the SH extratropical atmosphere. Dynamic response may include the weakening of mid-latitude surface westerlies, the expansion of polar easterlies further north and the slight strengthening and equatorward shift of middle tropospheric zonal jet, while the SAM had a positive phase tendency.

The use of ESMs in climate predictability, coupled interactions and process-oriented attribution studies is at its infancy stage and remains largely underexplored particularly in the context of SH climate variability. With this in mind, we revisited the topic using the Commonwealth Scientific and Industrial Research Organisation (CSIRO) Earth System Model (ESM) of intermediate complexity by placing more emphasis on the role of SIC, SST and coupled interactions on atmospheric leading modes of climate variability. The model's experiments, which consist of both idealised and comprehensive methods, are conducted in manner that decompose two scenarios: firstly, the contribution of sea–ice and ocean surface temperature through boundary forcing alterations, and, secondly, the isolation of the contribution of feedback mechanisms by allowing the model simulations to vary through coupled interactions.

The remainder of the paper is organised as follows: in Sect. 2 we describe the experimental design; we present results and discussions in Sect. 3; we provide a summary and conclusions in Sect. 4. Additional information is also provided in the form of electronic supplementary material.

Experimental design

Model description

The study uses the conformal-cubic atmospheric model (CCAM, McGregor and Dix 2008) of the CSIRO. The CCAM has recently evolved to the level of an ESM of intermediate complexity following its coupling with a dynamic ocean model (Thatcher et al. 2015), sea–ice model (Gordon et al. 2002; O'Farrell 2004) and biosphere model (Kowalczyk et al. 2013). The term intermediate complexity is used here from a context of hierarchy in terms of integrating interactively coupled components of the climate system and the coarse resolution adopted for the experiment to reduce the computational burden (Claussen et al. 2002). The manner in which the ESM experiment conducted resembles, to a large extent, the standard CMIP5 models configured for the purpose of comparison with observation (Taylor et al. 2012). The model's components and the coupling method are described next.

The atmospheric model makes use of the semi-implicit semi-Lagrangian time discretisation method to solve the hydrostatic primitive equation in a conformal-cubic grid projection and σ-coordinate system. It adopts the Geophysical Fluid Dynamics Laboratory (GFDL) parameterisations for long- and short-wave radiation with interactive cloud distributions determined by the liquid and ice-water scheme of Rotstayn (1997). The CCAM employs a stability-dependent boundary layer scheme based on Monin Obukhov similarity theory with the non-local treatment of Holtslag and Boville (1993). The cumulus convection scheme uses a mass-flux closure, as described by McGregor (2003), and includes downdrafts, entrainment

and detrainment. The model includes a prognostic aerosol scheme due to Mitchell et al. (1995) which can be applied consistently with the emission inventories and radiative forcing specifications of the CMIP5.

The CCAM runs coupled to a new generation sophisticated land-surface model referred to as the CSIRO Atmosphere Biosphere Land Exchange (CABLE) model (Kowalczyk et al. 2013). Over the last couple of decades, the model has developed from simple scheme to a complex representation of soil–vegetation–atmosphere interactions. It also incorporates biogeochemical knowledge and elements of the terrestrial carbon cycle, and becomes suitable for use in climate models. In addition, the CABLE model integrates a dynamic river routing scheme of Arora and Harrison (2007).

The sea–ice model, adapted from the CSIRO Mk3 Climate System Model (Gordon et al. 2002), consists of both ice dynamics and ice thermodynamics (O'Farrell 2004). In the model, hereafter referred to as the conformal cubic sea–ice model (CCSIM), grid points with sea–ice are also allowed to have part ice cover and part open water (i.e., leads/polynyas), with the ratio changing according to local conditions where the inclusion of the leads and open water promote better representation of the turbulent heat fluxes from the ocean to the atmosphere and the mixed albedo of the surface respectively.

The internal ice resistance that prevents ice from continually building up is parameterised using cavitating fluid rheology (Flato and Hibler 1992; O'Farrell 2004). Although a wide range of rheology schemes are available, a viscos–plastic rheology (Hibler 1979) with non-physical elasticity modification, also referred to as elastic–viscous–plastic (Hunke and Dukowicz 2002) is widely used in coupled sea–ice models (e.g., Xu et al. 2013; Rousset et al. 2015). As comparison studies (Flato and Hibler 1992; Schulkes et al. 1998; Kreyscher et al. 2002), suggest, the lack of shear induced deformation in cavitating fluid rheology may limit its ability to simulate attributes of ice motion or instabilities mostly found on high-shear zones. However, the choice between different ice rheologies in coupled climate models (ESMs) remains an open debate (Schulkes et al. 1998). The use of cavitating fluid rheology in the context of changes in concentration and future climate warming is found to yield reasonable results and balanced coupled simulations (Gordon and O'Farrell 2002; O'Farrell 2004).

The dynamic ocean, hereafter, referred to as the conformal cubic ocean model (CCOM, Thatcher et al. 2015) is a semi-implicit, semi-Lagrangian treatment of the primitive equations of motion using the Boussinesq and hydrostatic approximations. The coupler communicates the ocean and atmosphere models each time-step. In this process, the atmospheric model feeds the ocean model with momentum, radiation, heat and moisture fluxes. The ocean model, in turn, feeds information to the atmospheric model with SST. The approach is based on the reversibly staggered grid (McGregor 2005), which possesses excellent dispersive properties for modelling the geophysical fluid dynamics of both the atmosphere and the ocean. A common reversibly staggered grid (which is similarly applied to other model components of the ESM described above), eliminates the coupling overhead associated with message passing and makes the simulations computationally economical since it negates the need for interpolation in each model time step that is commonly applied in other coupled models to reconcile grid type and resolution among model components.

Model sensitivity experimentation

In the experiments described here, we use C48 quasi-uniform horizontal resolution (approximately 200 km) and 27 vertical sigma layers. Despite the model resolutions being relatively coarse to make the model simulations computationally feasible, the processes required to address the main objectives of the study are thought to be reasonably resolved.

The model experiments consist of four simulation strategies using forcing data from Climate of the Twentieth Century (C20C) provided through the CMIP5 (Coupled Model Intercompariosn Project Phase Six) archive for the period 1870–2014 (Folland et al. 2002; Rayner et al. 2003). Different model configurations are used aimed at decomposing, on one hand, the roles of sea–ice and ocean surface temperature forcings on climate variability, and on the other hand, examining the contribution of feedback mechanisms by allowing the model simulations to vary in coupled mode. In addition, all simulations are forced by the time-varying CO_2 and ozone fields. To minimise potential climate drift, the model is nudged at its surface to the CMIP5 AMIP boundary forcing, using the spectral nudging method of Thatcher and McGregor (2011). For convenience these experiments are, hereafter, referred to as *ESM*, *AMIP*, *SICclim* and *SSTclim* (see Table 1 for details). The ESM experiment is a coupled atmosphere–ocean–sea–ice–biosphere simulation, but with the ocean nudged at its surface to AMIP SSTs and SICs. The AMIP experiment is a standard AMIP simulation in which the atmosphere is forced at its lower boundary by inter-annually varying observed SSTs and sea–ice. In the SICclim and SSTclim experiments, climatological SICs and SSTs are used to replace the inter-annually varying fields. The ESM experiment is used here as a "control run" in order to expedite the sensitivity analysis. Because the ESM is (at least theoretically) expected to simulate the observed features of the climate system better than the other simulation strategies.

Observed data

The study uses observed data obtained from different sources. For the surface data, the boundary forcing noted earlier is used for trend and climate variability analysis in comparison to the ESM's SST and SIC simulations. For pressure data analyses, the National Centers for Environmental Prediction (NCEP) Reanalysis (R2) dataset (Kanamitsu et al. 2002) and the twentieth Century Reanalysis (20CR, Compo et al. 2008, 2011) are used as proxies for observation.

Results and discussion

Antarctica SIC and Southern Ocean SST variability and changes in recent decades

The results presented in this section focus on SH SST and sea–ice variability, and associated trends of recent decades. The leading modes of climate variability and trends are examined using the ESM simulations and objectively compared against observation. This modelling paradigm is used as a benchmark against which results from the model sensitivity experiments are to be compared (Sect. 3.2). Although we mostly confine the scope of our discussion on the trend analysis to the austral winter (June–July–August, JJA) and summer (December–January–February, DJF), as these two seasons represent the vicinity of opposite facets of the sea–ice seasonal variation, the sea–ice trend analysis during the austral spring (September–October–November) and autumn (March–April–May) is also presented in the supporting material (Fig. S1). Climatologically (shown as background in Figs. 1, S1), sea–ice

Table 1 Description of model experiment strategies and their configurations

Exp. ID	Description
ESM	Interactively couples atmosphere, ocean, biosphere and cryosphere models; nudged to time-varying AMIP SSTs and SICs
AMIP	Standard AMIP style simulation; interactively couples atmosphere and biosphere; forced with and nudged to time-varying AMIP SSTs and SICs
SICclim	As "AMIP" except forced with and nudged to AMIP SIC climatology
SSTclim	As "AMIP" except forced with and nudged to AMIP SST climatology

All experiments use AMIP sea-surface temperatures (SSTs) and sea–ice concentrations (SICs) provided through CMIP5 as a lower boundary forcing or nudging

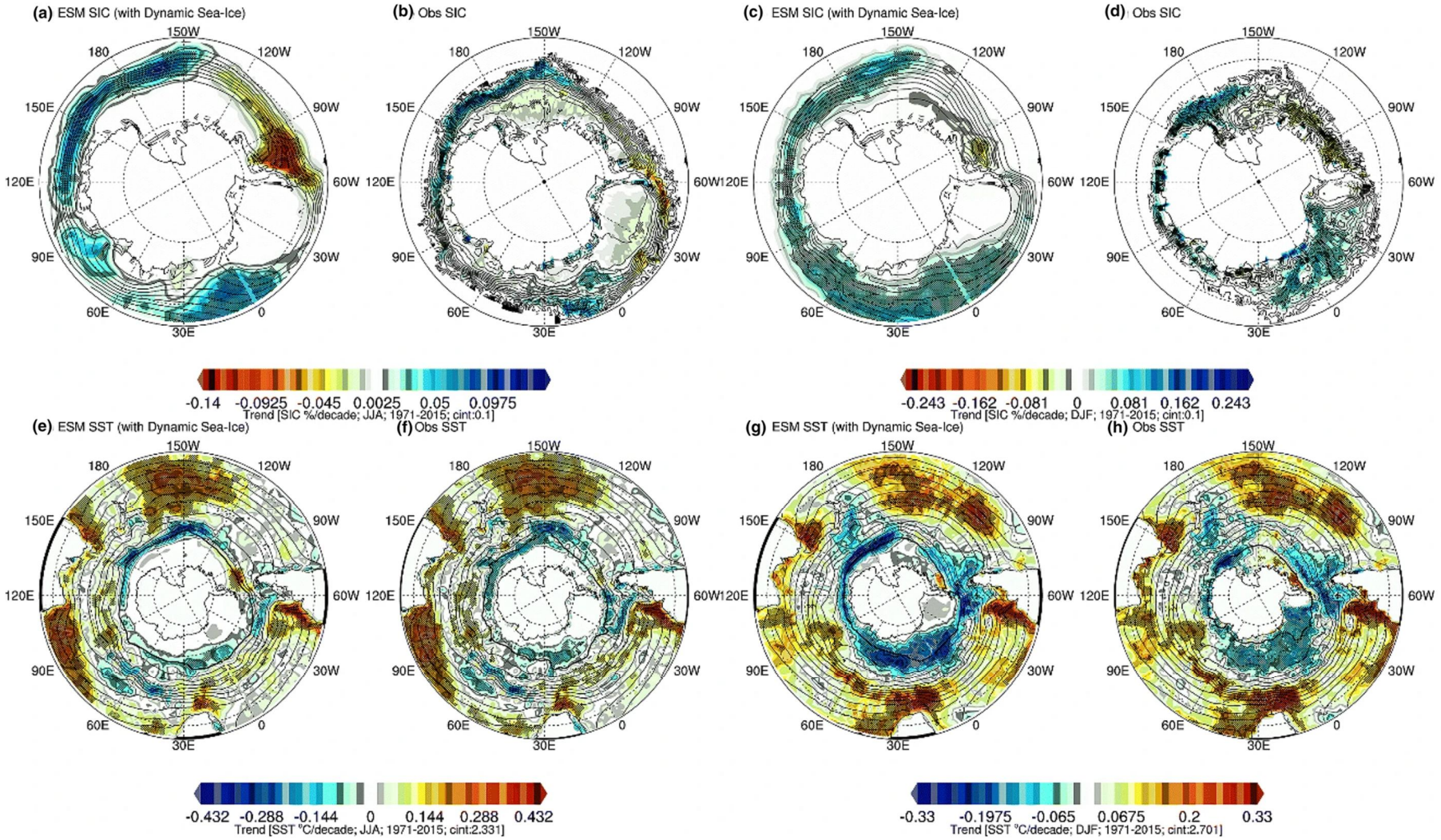

Fig. 1. Modelled and observed linear trends (per decade) SH SIC (upper panel) and SST (lower panel) during the austral winter (**a**, **b**, **e**, **f**) and summer (**c**, **d**, **g**, **h**) for the period spanning 1971–2015 as shown in the title of each plot. Regions with statistically significant trends at 95% are indicated with stippling

starts forming in the austral autumn and continues growing throughout winter, reaching its maximum in September. It starts retreating (melting) in October through December and January. Relatively cool SSTs are observed further south, near Antarctica, and relatively warm SSTs are observed to the north of the Antarctic Continent.

The linear trends are estimated using the non-parametric Mann–Kendall and Sen methods (Hamed and Ramachandra Rao 1998; Gocic and Trajkovic 2013). According to Fig. 1, the Southern Ocean displays, to a large extent, a warming trend over the mid-latitude, but with a cooling trend in SSTs over the SH circumpolar belt off the coast of Antarctica. The latter change apparently coincides inversely with the SIC trend at the ocean–sea–ice interface, which is pronounced during the austral summer (Fig. 1h, g). Furthermore, the Southern Ocean warming crests tend to co-occur with the centres of anticyclones (see Fig. 2 in Pepler et al. 2018), with this feature consistently represented in both the model simulations and observations. During the austral winter, the change is seen with extended spatial extent over the south-eastern Indian Ocean and southern Pacific Ocean. Anticyclones vary in phase with the strength and intensity of the local mean subtropical ridge, with anticyclone variability also associated with the SAM (Pepler et al. 2018). In fact, the result is consistent with the SAM's tendency toward positive polarity over recent decades (Marshall 2003; Jones et al. 2016), as we see in detail in subsequent sections.

The spatial linear trend analysis also reveals that the ESM simulations and observations share a great deal of resemblance in their representation of the SIC and SST trends over the Southern Ocean south of the 45° latitudinal belt. This may be attributed, at least to some extent, to the spectral nudging technique of Thatcher and McGregor (2011), by which the model SSTs and SICs were nudged toward the AMIP observations. However, the nudging is indirectly applied to the sea–ice in the model simulations. To maintain some agreement with sea–ice in the host model, we nudge the surface temperatures to the freezing point where sea–ice is present. This encourages the formation of sea–ice if the ocean temperatures are not already at the freezing point (i.e., in cases where sea–ice is absent). This approach also encourages melting of the model sea–ice for locations which are not in the host model due to encouraging temperatures above the melting point. In this way, the ESM sea–ice has some freedom to deviate from that of the host model, since it is not directly prescribed by the nudging but instead encouraged by the nudging of ocean temperatures.

Figure 2 presents the SH SIC and SST leading rotated empirical orthogonal functions (EOFs, Mestas-Nuñez 2000). The spatial coverage for the latter is expanded south of 25° S to account for mid-latitude variability. The analysis is based on the monthly mean of all calendar months of each field which is subjected to least squares quadratic detrending. Nonlinear detrending is chosen because it reasonably removes monotonic trending (Wu et al. 2007) as also confirmed here (not shown). The EOF patterns are normalised by their respective eigenvalues in order to bring their amplitude to the same space. The first sea–ice dominant mode, explains 11.5% (model, Fig. 2a) and 7.2% (observation, Fig. 2d) of the variability, and again reveals the dipole-like sea–ice pattern. The other modes of observations more or less display a similar pattern with slight zonal shift in orientation. While the first two leading modes of the model simulations have a similar amplitude structure with their respective observations, the last mode of the model has two troughs over the Ross Sea and the southern Indian Ocean off the coast of Antarctica which are not present in the observed mode. By and large, the appearance of the dipole-like sea–ice pattern in the leading observed modes suggests the importance of the underlying physical processes associated with the sea–ice.

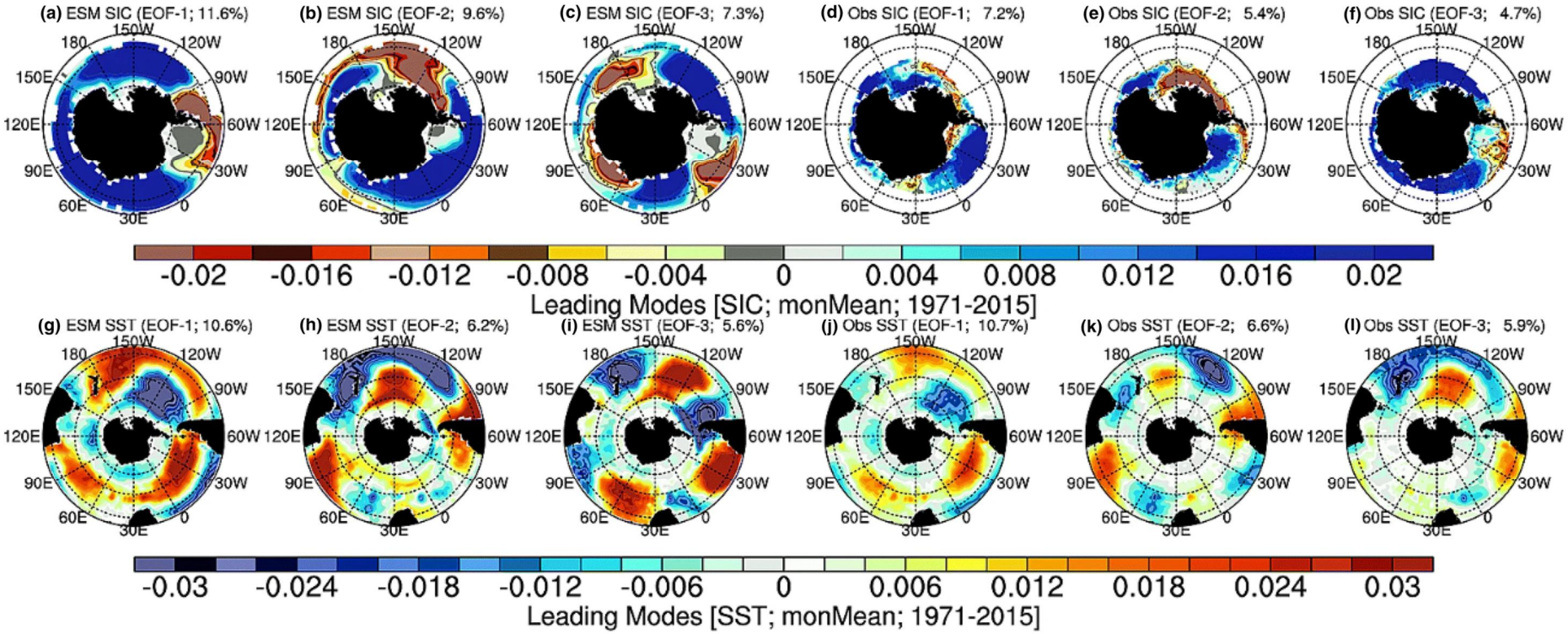

Fig. 2. Simulated and observed first three leading SH SIC (upper panel) and SST (lower panel) modes of variability based on the (rotated) EOF analysis using detrended monthly anomaly of each field as input. Also shown in the title of each plot is the EOF mode rank along with its variance explained (%)

The modelled and observed first leading mode of Southern Ocean monthly SST anomalies share similar spatial patterns and extent of variance (Fig. 2g, j). This most dominant SST variability, which the largest amplitude in the Pacific sector, resembles the annular mode (Wang and Dommenget 2016). Notwithstanding, the order of the other two modes in the model are swapped, i.e., EOF-2 (EOF-3) of the observation is spatially coherent with EOF-3 (EOF-2). These modes are characterised by wave-train like patterns with slightly different spatial structures where the previous pair consists of three and four clear crests and troughs respectively, whereas the latter pair has a zonally elongated trough with three crests (Fig. 2h, l). However, all the simulated leading modes tend to have pronounced spatial loadings (eigenvalues) compared to the observations. As Wang and Dommenget (2016) have pointed out, the annular mode at interannual to decadal timescales is strongly related to atmospheric forcing by the SAM and ENSO. Furthermore, the second mode has pronounced multi-decadal and longer time scales variability, which presumably, relate to the wave-3 patterns in the atmosphere and the ocean. The third mode gradually transforms from a wave-train pattern to a dipole structure in the Pacific at longer timescales.

Noteworthy is the dominance and deepening of the dipole-like sea–ice pattern between the Ross Sea and the Amundsen–Bellingshausen–Weddell Sea sector in the EOF and trend analyses respectively. According to Figs. 1 and S1, the Antarctica sea–ice dipole pattern deepening is a year-round phenomenon. The finding may suggest the presence of (or need for) an equivalent mechanism to sustain.

It is worth clarifying, however, the manner in which the term *deepening* and *dominance* of the dipole-like sea–ice pattern (Antarctic dipole) are used here. The former implies the amplification and depletion of SIC on the Ross and Amundsen–Bellingshausen–Weddell Seas respectively from the trend analysis perspective. The latter refers to the hierarchy of the dipole from the EOF analysis perspective. Li et al. (2014) have attributed the deepening aspect to the AMO, which tends to reduce the surface pressure in the Amundsen Sea. However, the AMO's modulation is exclusively restricted to the austral winter due to tropical Rossby wave trains being trapped in the Atlantic sector during the austral summer. Despite this, ENSO may also be inducing a similar response (Turner 2004; Yuan 2004), arguably to act in synergy with SAM or PSA to strongly influence the Antarctic climate (Fogt and Bromwich 2006; Stammerjohn et al. 2008; Pezza et al. 2012). Nonetheless, it is unclear whether the Pacific SST variability explains the Antarctic multidecadal climate changes as ENSO is an interannual climate mode.

We extended our analysis on the SIC (Fig. 3) and SST (Fig. S4) simulations of the ESM using the mean-square skill score (MSSS; Murphy 1988). The MSSS is an actual measure of skill due to its sensitivity to model biases, and thus represents improvement in the model's ability to simulate observed features relative to a reference (here we use climatology as a reference, Beraki et al. 2014). The reflection of this sensitivity is also apparent in the fact that the concentration of skill (e.g., Fig. 3a–d) corresponds with the low error concentration (e.g., Fig. 3e–h) for all seasons. The MSSS has a value of one for perfect forecasts and zero for no improvement relative to the climatology. It could be positive (negative) when the accuracy of the forecast is superior (inferior) to the accuracy of the climatology. According to Fig. 3, the ESM is able to show useful skill particularly during the austral spring and summer seasons. The model's ability to simulate the SH, particularly over most parts of the Southern Ocean for all seasons, SST is high. Notwithstanding, the model has shown a mixed signal over the circumpolar region where it has a superior (inferior) concentration of skill to reference in all seasons, except the austral spring.

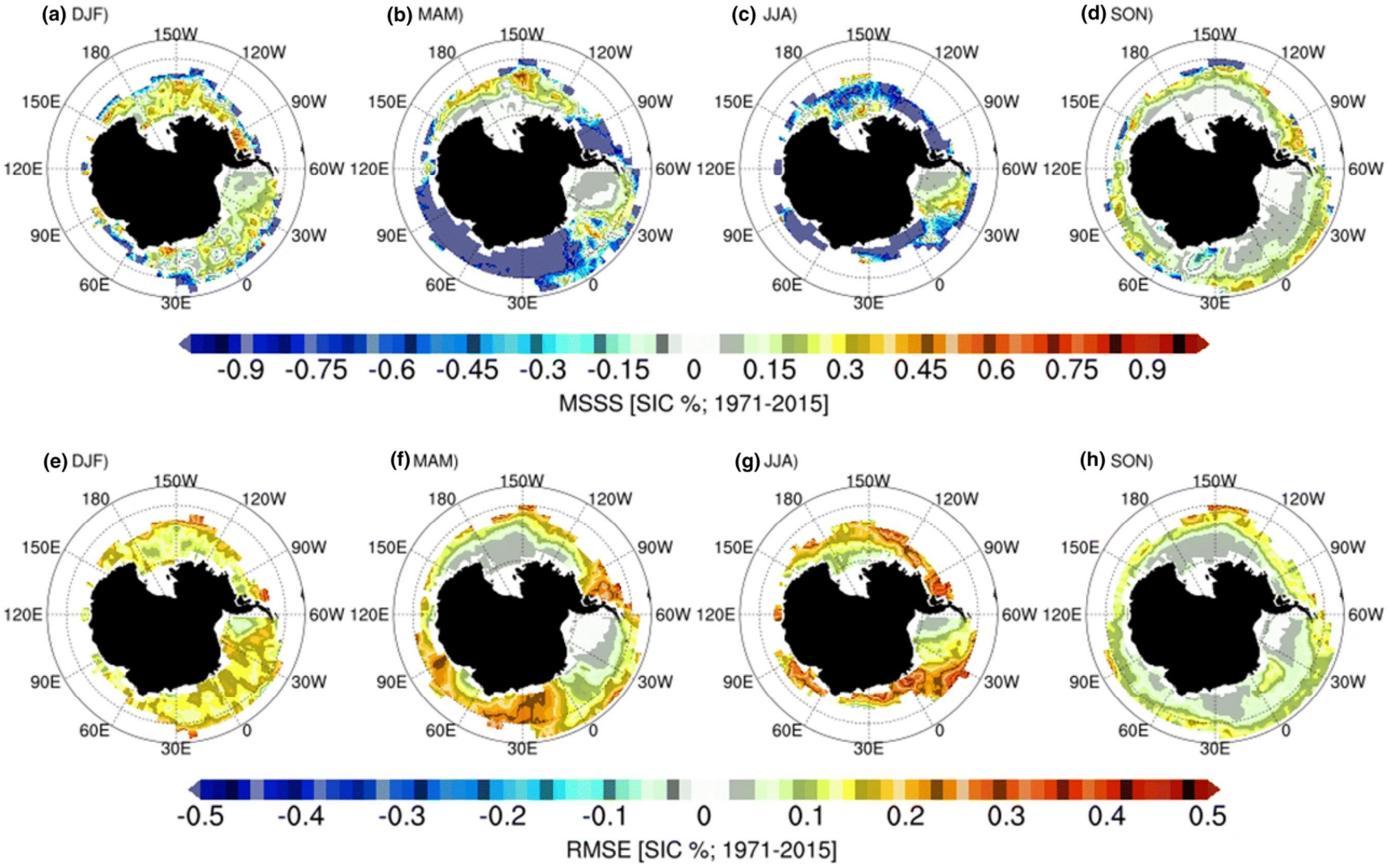

Fig. 3. ESM actual skill and level of accuracy simulating observed SH SIC using MSSS (top panel) and RMSE (bottom panel) respectively for the four main seasons. Regions with statistically significant MSSS at 95% are indicated with stippling. The significance test is performed using bootstrap none parametric technique (resampling with replacement for ×1000)

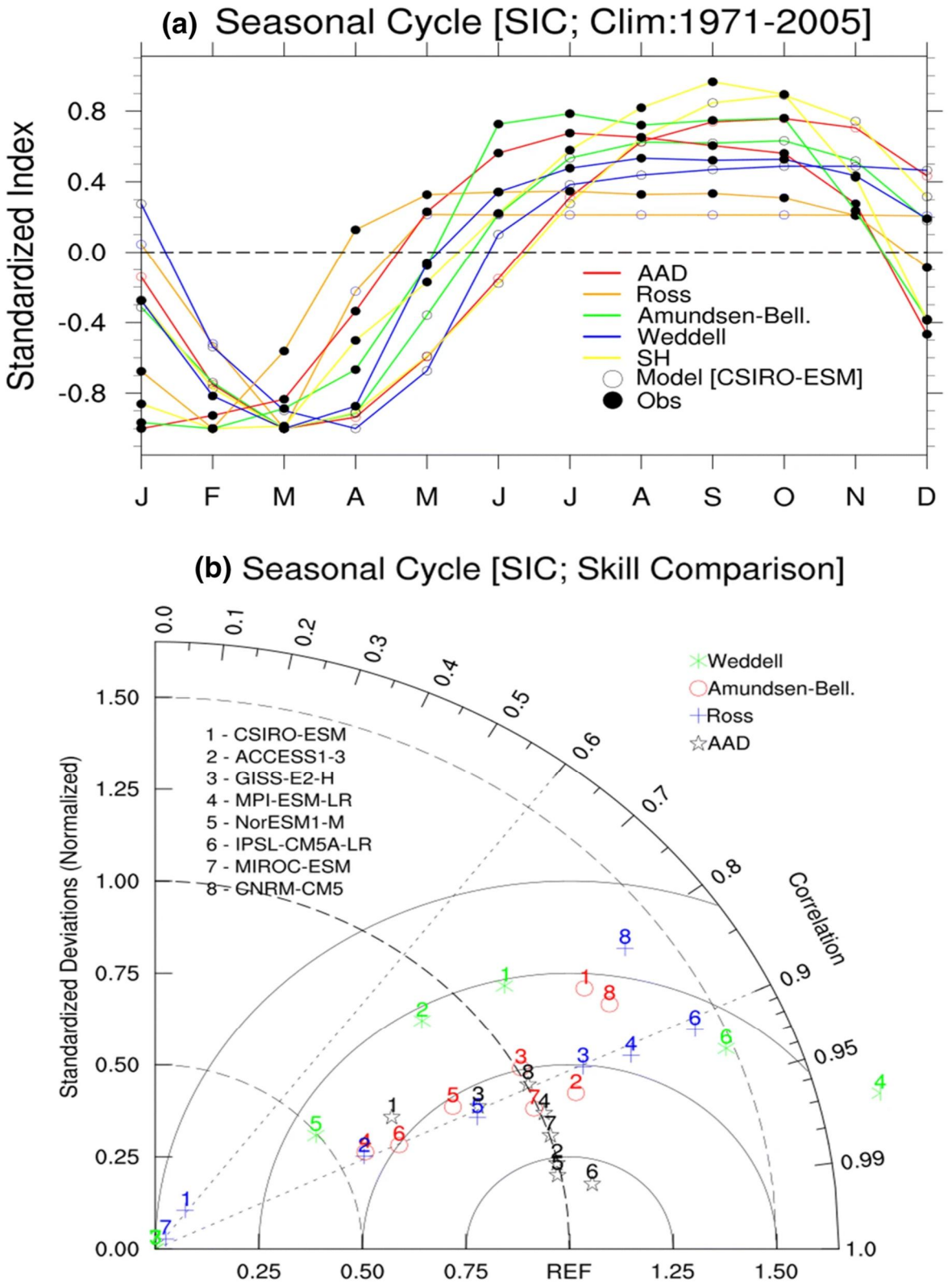

Fig. 4. SH SIC seasonal cycle for various sea basins. The indices are rescaled (normalised) to bring them is within the same space to expedite the comparison among indices representing various sea basins off the coast of Antarctica; (**a**) seasonal cycle climatology of the ESM and (**b**) seasonal cycle skill among various models (Taylor Diagram, Taylor 2001) against AMIP observation, as shown in the inset of each plot. The AAD index is deduced from the first EOF Analysis by projecting the respective SIC monthly climatology of each model. The indices for the other sea-basins area average within ± 5° centered locations [Ross Sea (74.5487° S, 166.3074° W); Amundsen–Bellingshausen seas (62 12° S, 58.56° W); Weddell Sea (71.1879° S, 45.00° W)]

The ESM representation of the SH SIC seasonal cycle has also been investigated (Fig. 4). The assessment uses various indices representing the Antarctic sea–ice dipole (AAD), the Ross Sea, the Weddell Sea and the Amundsen–Bellingshausen Sea. According to Fig. 4a, our ESM (denoted as CSIRO-ESM) is able to simulate the observed asymmetric seasonal cycle of the Antarctic sea–ice with a tendency of 1 month phase error. As shown in Fig. 4b, the model seasonal cycle of AAD is also compared with a suite of CMIP5 climate models historical simulations (Taylor et al. 2012). The comparison suggests that the CSIRO-ESM and CMIP5 Climate models (considered in the analysis) are successful in representing the AAD seasonal cycle as measured using the Spearman rank order correlation despite the intermodel seasonal cycle being found to be highly variable. The time series analysis further suggests (not shown) that the CSIRO-ESM is more skilful in simulating the low-frequency AAD trajectory than the CMIP5 models under consideration.

Interannual and multi-decadal atmospheric response

In the following analysis, we focus on atmospheric circulation variability and its low frequency response to various climate forcings. Figure 5 shows the SH monthly mean of 700 mb geopotential height (GH) anomalies leading (rotated) EOFs for each simulation strategy (Table 1). As with the SSTs and SICs, GH is subjected to least squares quadratic detrending to remove monotonic trending. The variances explained (eigenvalues, shown in the title of each plot in Fig. 2) by the first three EOF patterns are well separated as tested using the rule of thumb for estimating sampling error (North et al. 1982). The first mode represents the dominant atmospheric variability, commonly referred to as the SAM or the Antarctic Oscillation (AAO). The structure of the SAM, which is represented with the spatial loadings (normalised eigenvalues) in the model experiments and reanalyses, are consistently similar. The SAM is a largely zonally symmetric atmospheric structure with pressure anomalies of opposing signs vacillating between the polar and mid-latitudes of the SH (Limpasuvan and Hartmann 2000; Thompson and Wallace 2000). The SAM is an inherent part of the climate system with significant ocean and sea–ice interactions. The anomalous SAM tends to affect the westerly circumpolar flow, and then further influences the circulation, temperature distribution, mixed layer depth and heat capacity in the ocean through the Ekman pumping effect (Hall and Visbeck 2002; Lefebvre et al. 2004; Sen and England 2006; Yuan and Li 2008).

The other SH leading modes also generally exhibit a great deal of similarity (Fig. 5). However, the EOF-3, which resemble a wave like train (wave number 3; Wang and Dommenget 2016), shows some differences in their (normalised) eigenvalue patterns. The SSTclim simulation, for example, has an amplified trough in the south western Atlantic and southern Indian Oceans (EOF-3, Fig. 5p); these features are either non-existent or have eastward displaced shallow trough in the other simulations. The other difference is that the SICclim atmosphere has relatively stronger south Pacific and south Atlantic crests (Fig. 5o) than its AMIP counterpart (Fig. 5n). These sensitivities, presumably, suggest that the sea–ice forcing, to some extent, plays a role in modulating the atmospheric variability locally (Morioka et al. 2017).

To examine how the leading modes have evolved at various timescales, we consider two periods: one representing the years spanning 1871–2015 (20CR) and the other representing years from recent decades (1979–2015, Fig. 6). The latter is consistent with the period used in the trend analysis throughout the study and the aim of zooming in on this period is to scrutinise the sensitivity of interannual atmospheric variability better, while the former

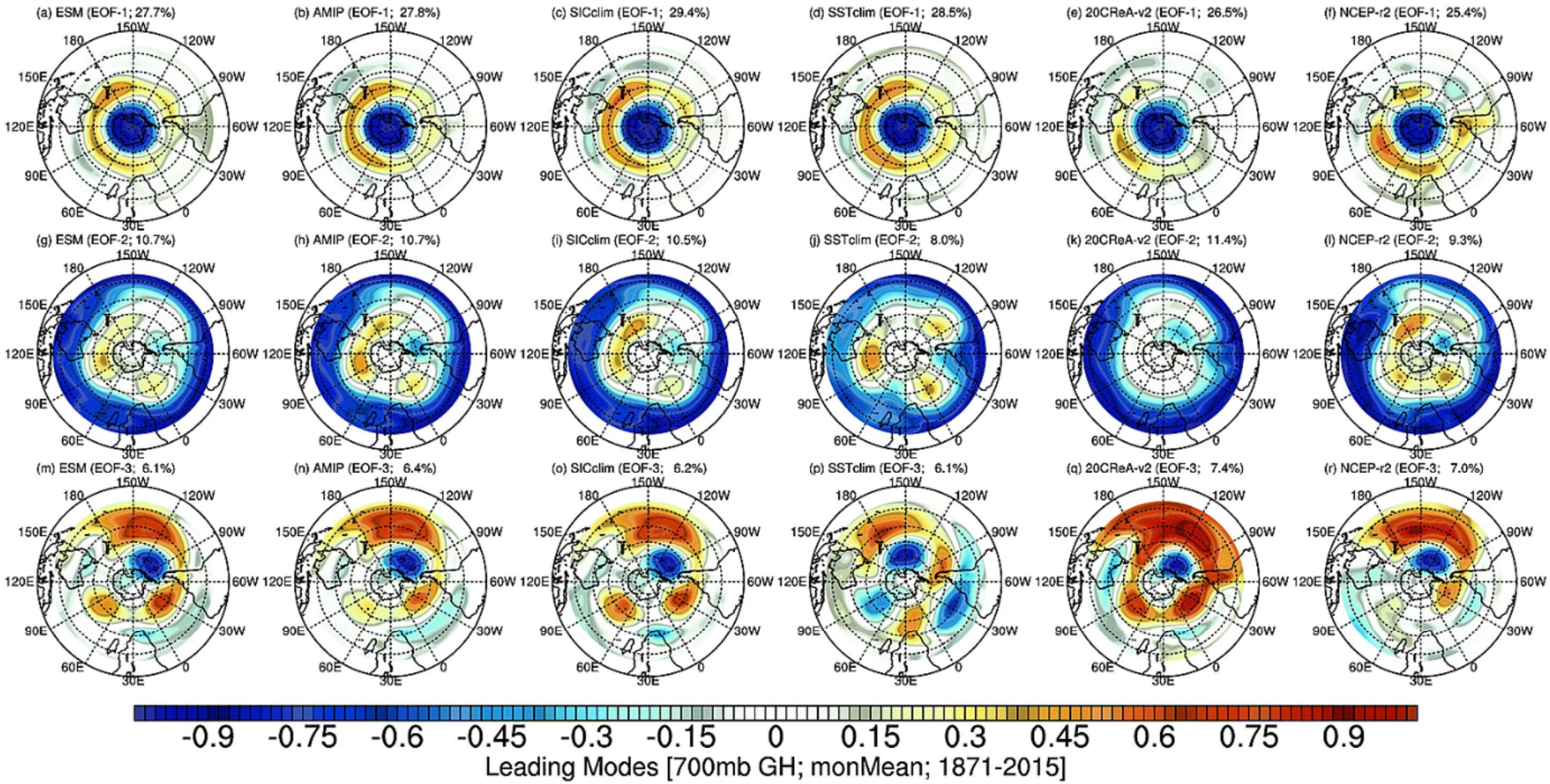

Fig. 5. Simulated and observed three most leading SH 700 mb GH modes of variability based on (rotated) EOF analysis using detrended monthly anomalies emanated from the four model experiments (Table 1) and two sources of observations as shown in the title of each plot along with the variance explained (%)

explores the multidecadal or low frequency atmospheric variability response to different forcings. According to Fig. 6, the time evolution of the SAM is chaotic and follows a random trajectory (across the simulations) at the interannual timescales. This dynamic behaviour is poorly reflected in terms of coherency and goodness of fit, measured using the Spearman ranked correlation and root mean square error (RMSE) respectively showing on the inset of Fig. 6. The skill scores for AMIP, SICclim, SSTclim experiments and observations were calculated against the ESM (used as a benchmark as noted above).

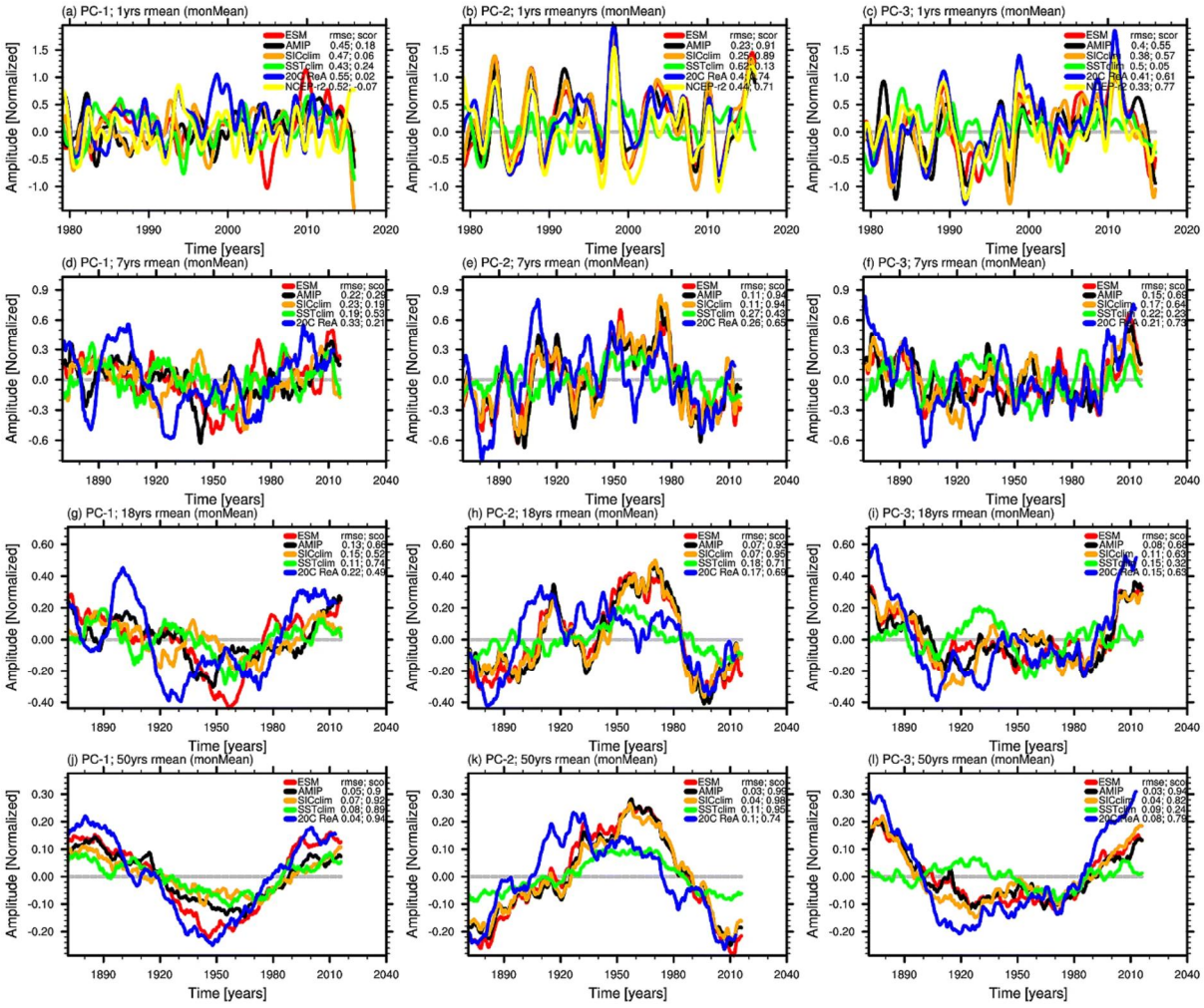

Fig. 6. The leading principal components (PCs) of SH 700 mb GH, which show how the corresponding leading EOF modes (Fig. 5) evolve at interannual and multi-decadal timescales. Also shown in the inset of each plot is a spearman correlation and root mean square error (RMSE) as measure of coherency and goodness of fit respectively relative to the ESM (control simulation)

Notwithstanding, there is a pattern of increasing consistency across the different simulations in representing the temporal evolution of the SAM (Fig. 6g, j) as the timescale increases. In fact further smoothing (Fig. 6j) surprisingly unveils, on one hand, the sensitivity of the SAM to sea–ice and SST forcings and, on the other hand, the extent to which the AMIP experiment suffers further divergence from the 20CR relative to the ESM simulation. This suggests that multiple feedback mechanisms arising from the coupled interactions noticeably modulates the time-evolution of the SAM. There are two plausible explanations that support the notion. First, the difference between the AMIP and ESM configurations is only in the manner in which the ocean, sea–ice and atmosphere interact with one another while the two systems

remain nearly identical in other aspects. Second, the AMIP, SSTclim and SICclim experiments exhibit a tendency to cluster, which suggests a lack of noticeable independent sensitivity to SST or SIC forcing.

The other leading modes exhibit a high degree of consistency except in the SSTclim scenario which tends to oscillate quite differently. This noticeable sensitivity emphasises the importance of (notably tropical) ocean temperature forcing irrespective of timescales. However, the SIC climatological forcing (SICclim) is indistinguishable from the ESM and AMIP experiments, suggesting that sea–ice forcing does not seem to play a significant role in driving these modes of climate variability or influencing a hemispheric-wide atmospheric response.

As a leading atmospheric activity in the SH mid-latitude, the SAM signature is significantly felt on the regional climate through air-sea interaction (Limpasuvan and Hartmann 2000; Thompson and Wallace 2000), for instance, in South America (Silvestri and Vera 2003), Australia (Feng et al. 2010), New Zealand (Kidston et al. 2009) and South Africa (Reason and Rouault 2005). As many studies indicate (e.g., Thompson and Wallace 2000; Swart and Fyfe 2013), the positive phase of the SAM, for example, is associated with the poleward shift of storm tracks over the Southern Ocean. Thus, any model success in simulating the low frequency oscillation of the SAM, with the prospect demonstrated here particularly with the use of the ESM (Fig. 6j), may have positive implications for downstream predictability such as mid-latitude storm tracks and austral winter climate variability that affects the southern Africa subcontinent, as well as other regions noted above. Such prediction has been found to be largely elusive in current-prediction systems due to the chaotic nature of inter-annual variability in the mid-latitudes, as described earlier. Furthermore, the analysis strengthens the notion that the subseasonal to interannual prediction of the SAM is presumably unachievable even with the use of ESMs, although our finding is based on one ESM. The fact that the two sources of reanalysis have inconsistent representation (Fig. 6a) also serves as a proxy indicator confirming the chaotic nature of the SAM at this timescale.

Recent changes on atmospheric response and possible causes

So far, we have examined the response of SH atmospheric (circulation) variability to various climate forcings. In light of the recent trends recorded in SICs and SSTs presented in Sect. 3.1, it is of interest to explore whether the atmospheric circulation also showed significant trends over the last few decades. If such trends do exist, the next question would be around identifying the mechanisms responsible for the trends. In order to answer these questions, we subjected the observed and simulated geopotential fields at different pressure levels to trend analysis. The linear trend and significance tests were computed as noted above using the non-parametric Theil–Sen estimator and Mann–Kendall respectively.

The trend analyses focus on SH surface and upper air circulation features including the polar vortex (tropospheric circumpolar trough; Jones and Simmonds 1993; Waugh et al. 2017) and sub-tropical high pressure regime (anticyclones; Pepler et al. 2018). Atmospheric sensitivity to global SST forcing remains conspicuous for the seasons considered over the analysis period based on the trend analyses applied to mslp and GH at different levels stemmed from the sensitivity experiments (Figs. 6, 7, S2, S3). One major sensitivity in the SSTclim experiment during the austral winter is that the strengthening of the polar mslp, which, in turn seemingly weakens the tropospheric polar vortex. Nonetheless, the sub-tropical high-pressure regime has remained nearly unchanged in contrast to the other experiments and observations

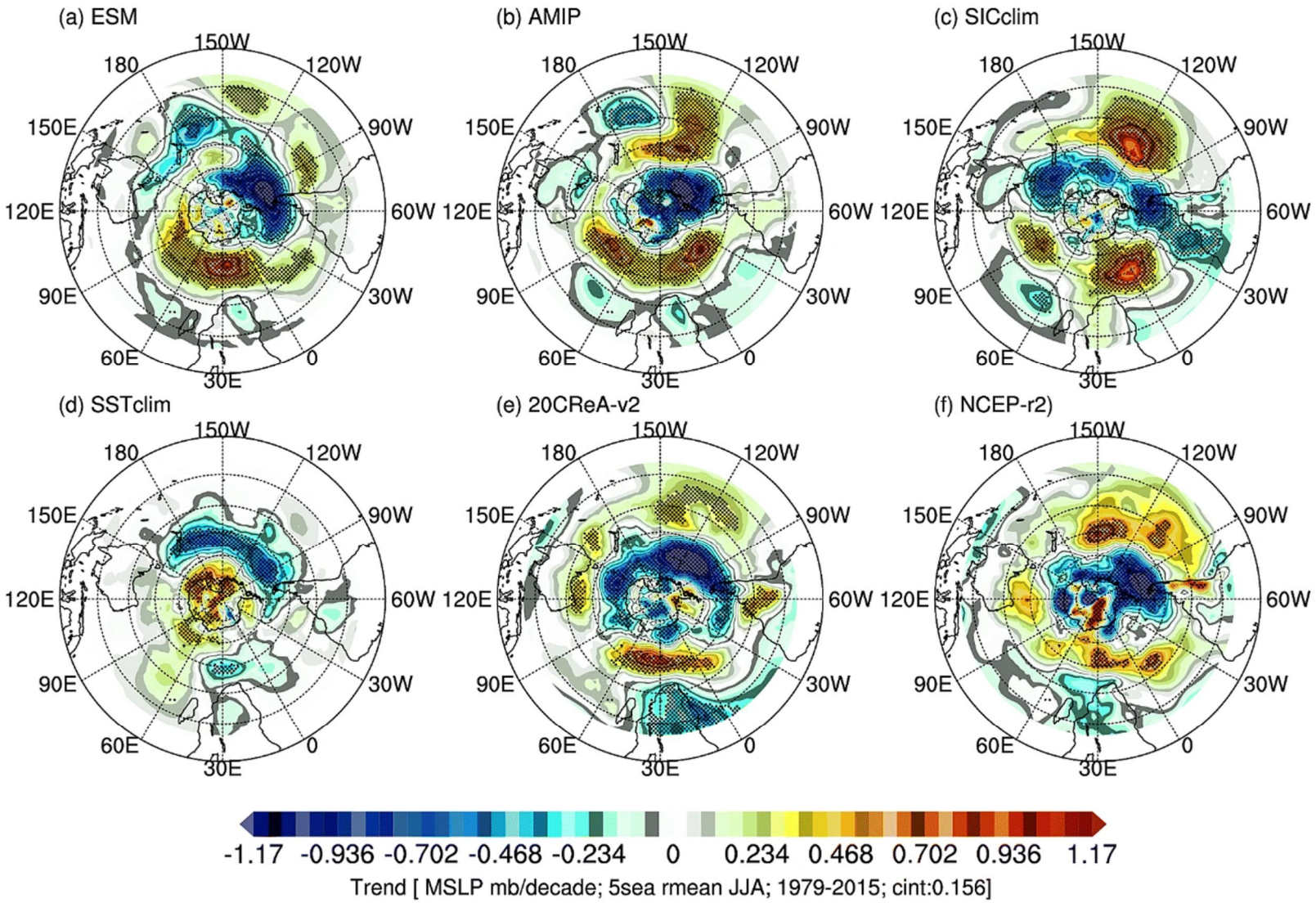

Fig. 7. Simulated (**a**–**d**) and observed (**e**, **f**) linear trends of SH mid- and high-latitude mslp mb/decade, during the austral winter. Regions with statistically significant trends at 95% are indicated with stippling

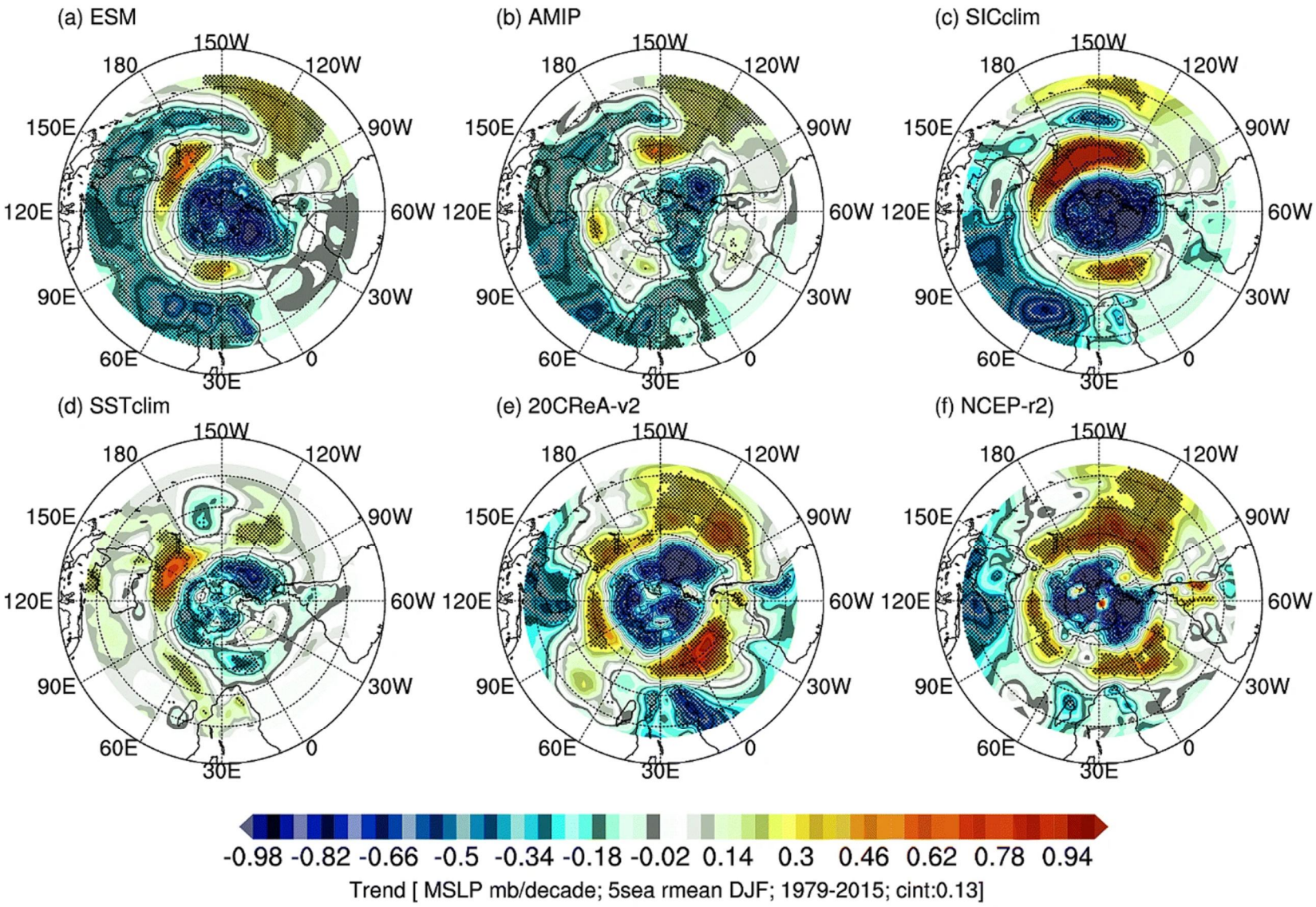

Fig. 8. As Fig. 7 but for austral summer

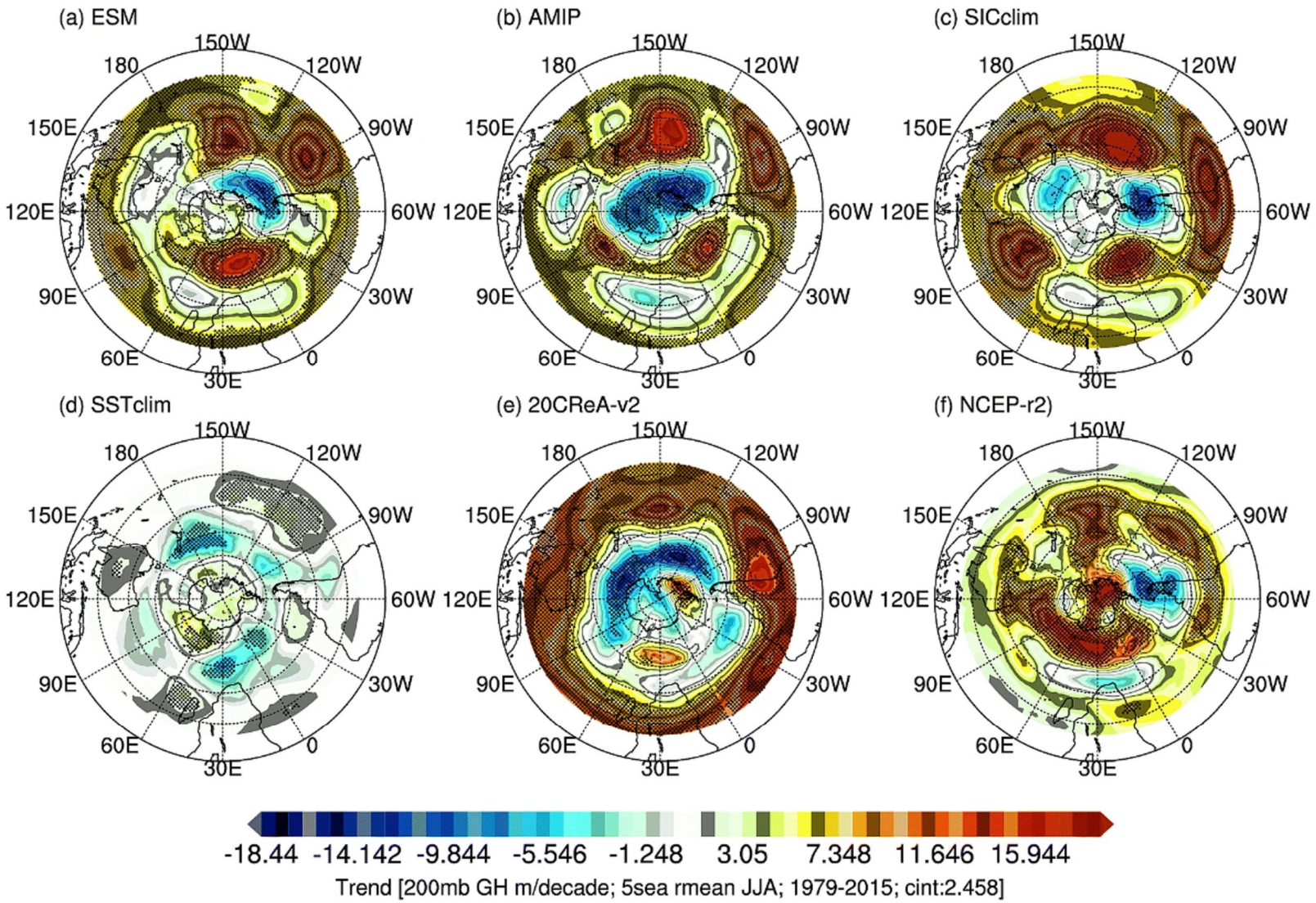

Fig. 9. Simulated (**a**–**d**) and observed (**e**, **f**) linear trends of SH mid- and high-latitude 200 mb GH m/decade, during the austral winter. Regions with statistically significant trends at 95% are indicated with stippling

(Fig. 8). In addition, the sensitivity to SST forcing has amplified in the upper air where the polar and mid-latitude circulations have significantly reduced (Figs. 9d, S2d, 3d). This noticeable sensitivity arises from the degradation of SST forcing to climatology is apparently an indication of sea–air coupling phenomena over the polar and mid-latitude regions. Recent studies (e.g., Minobe et al. 2008; Czaja and Blunt 2011) suggested the role of moist convection in upward transferring of oceanic conditions throughout the troposphere. Furthermore, this out-of-phase pattern, which presumably defines the phases of the SAM, is swapped in the other experiments and observations (Figs. 9, S2, S3). This drastic difference in the spatial trends, to the extent of altering the orientation and organization of the polar and mid-latitude pressure regime, suggests that changes in SST forcing is an important source of atmospheric variability, and likely explains the associated changes and the tendency of the SAM towards positive polarity over the last few decades as noted earlier. As a leading mode in the SH, the SAM describes the state of key pressure regimes (gradients), atmospheric flow and associated cyclogenesis activities that happen at the northern edge of the circumpolar trough (55°–65°) and their trajectories. The SAM phases play major role in shaping how these atmospheric features evolve in space and time. Its positive phase, for instance, substantially weakens the westerlies and shrinks the spatial extent of the polar vortex. Its positive phase, in contrast, effect equator-ward expansion of westerlies and weakening of the tropospheric polar vortex. The latter increases the likelihood of more cases of storms developments and their penetration to the southern part of Australia and Southern Africa sub-continent during austral winter (Hall and Visbeck 2002).

Notwithstanding, the changes presumably attributed to sea–ice forcing are mostly restricted to the vicinity of the sea–ice–air interface. Moreover, such changes are relatively deeper over the southern Pacific and Atlantic sectors. Furthermore, an equatorward incursion of the circumpolar trough (polar vortex) towards the mid-latitudes over southern South America is only seen in the SICclim experiment (Fig. 8c). This tendency is also present in the lower levels of the GH (Fig. S2) but gradually decays in an upward direction (Figs. 7c, S3c). Nonetheless, this feature may not have any correspondence to reality, given the lack of signal on the other experiments or observations, which negates its importance. The results might suggest that most of the changes seen in recent decades are marginally explained by sea–ice forcing and that the sea–ice impact on atmospheric circulation is highly localised in nature.

For the austral summer, the SH atmospheric circulation has also undergone statistically significant changes. Most of the model simulations and observations consistently indicate the intensification of the polar vortex and mid-latitude anti-cyclones. Also shown is the deepening of extratropical low-pressure regime specifically over the Indo-Pacific sector albeit slightly exaggerated in the model (Fig. 7). Nonetheless, the pattern is reduced to polar and mid-latitude upper level symmetric out of phase flow (Fig. 10). This intensification suggests the dominance of positive phase of the SAM over the last three decades. In the SSTclim atmosphere, not only is the change on low level atmospheric calculation over the polar and mid-latitude noticeably weakened relative to observations and the control simulation but the intensification of the extratropical pressure regimes, is also absent (Fig. 7d). In the upper air circulation (Fig. 10), while the polar vortex strength remains comparable, the mid-latitude vacillation is within the natural variability limit (Fig. 10d). In the SICclim atmosphere (Fig. 7c), the near-surface deepening of the polar vortex and Pacific mid-latitude anticyclones are stronger relative to the other experiments and observations (Fig. 7). The changes in the upper air circulation are comparable across the simulations, except in the AIMP and SSTclim experiments where the sensitivity of atmospheric circulation is apparent (Fig. 10b, d).

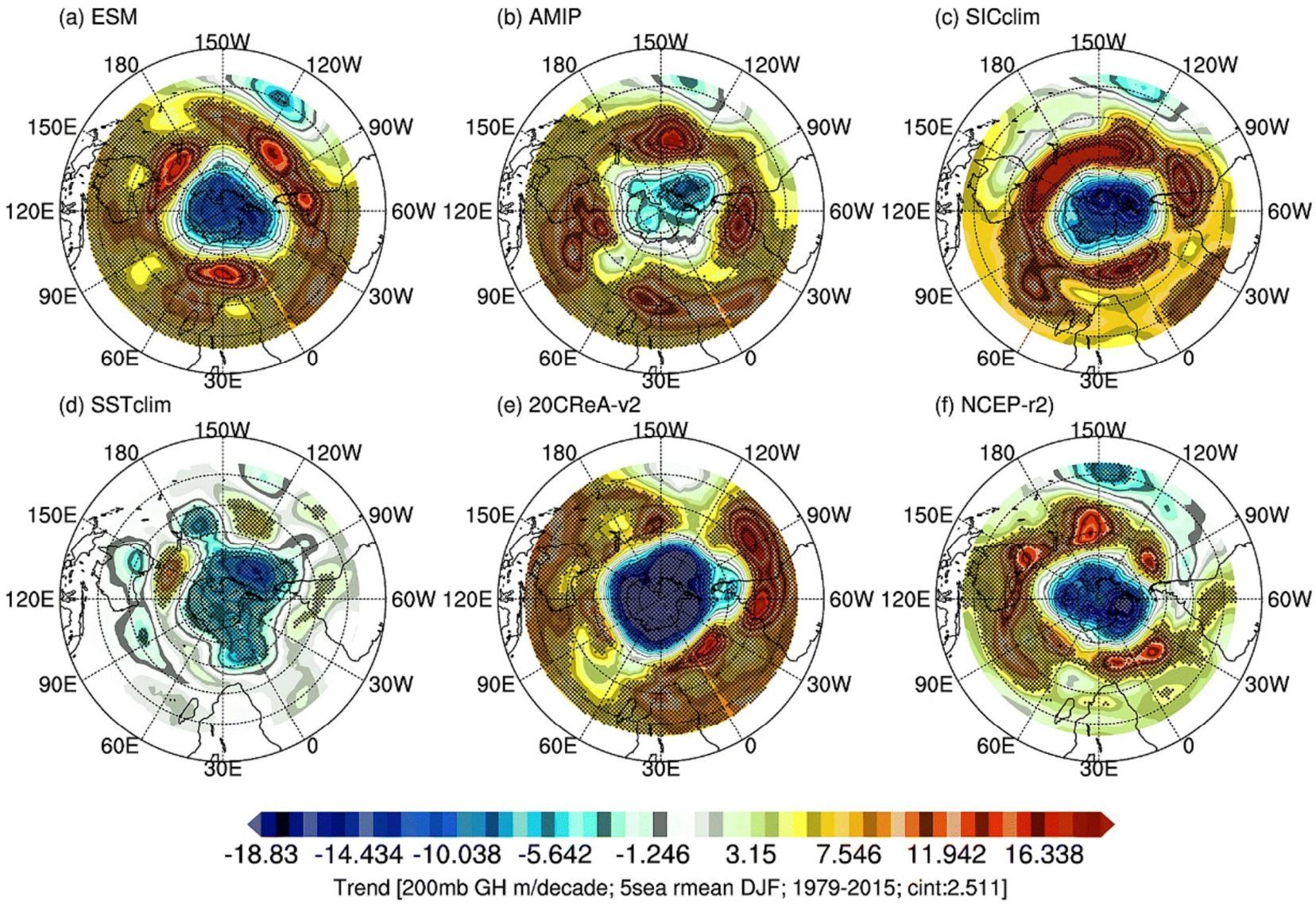

Fig. 10. As Fig. 9 but for austral summer

What transpires from our findings is that most of the noted changes are possibly explained by the SST changes although the sea–ice forcing also induces some level of sensitivity (largely confined within the vicinity of the sea–ice–air interface or low-level atmospheric circulation). In addition, the atmospheric circulation is also found to be sensitive to multiple feedback mechanisms that arise, to some degree, from the climate interactions. One probable justification is that the tropospheric polar vortex (Waugh et al. 2017) signal is substantially reduced during the austral winter in the AMIP experiment (Fig. 10b) in comparison with the ESM experiment (Fig. 10a). This suggests that the local air-sea–ice interaction seemingly acts to dampen the atmospheric variability in the model world, although this is unclear in the real world. As explained in Sect. 2.2 (Table 1), the main difference between the AMIP and ESM experiments resides on the manner in which the SST and SIC are represented while they are kept similar in all other aspects. Differences in this regard is attributed to multiple feedback mechanism, which is solely found in the ESM experiment.

It is also important to emphasise that the trend analysis was applied only over the last few decades. We were unable to trace any significant changes when the analysis period considered the period before the 1970s.

Summary and conclusions

The contribution of various climate forcings and their complex interactions is arguably believed to embrace untapped sources of climate predictability. ESMs are useful instruments to advance our understanding of aspects pertaining to climate predictability, coupled interactions and process-oriented attributions. With this in mind, the study exploits the utility of using the CSIRO-ESM to build a numerical experimentation that encompasses both idealised and comprehensive methods. In this regard, the study has investigated the influence of SIC and SST forcings, and atmosphere–ocean–sea–ice coupled interactions on the SH leading modes of climate variability and recent changes. The ESM simulations, used as benchmarks, have also been evaluated within the context of the Antarctic sea–ice and Southern Ocean SST variabilities and trends.

Our findings indicate the dominance and deepening of the dipole-like sea–ice pattern which is characterised by the respective amplification and depletion of SIC on the Ross Sea and Amundsen–Bellingshausen–Weddell Sea sector. Although previous studies (e.g., Turner 2004; Yuan 2004; Li et al. 2014) have suggested that the AMO and ENSO modulations were the main mechanisms inducing this dipole-like sea–ice changes, given the dipole-like sea–ice pattern's year round deepening tendencies, we hypothesise that a perpetual mechanism is presumably essential to sustain its maintenance. Another plausible possibility is that the change is part of the multidecadal or longer timescale intrinsic variability, which may be explained by feedback mechanisms that arise from coupled interactions (e.g., Hall and Visbeck 2002; Wang et al. 2014; Turney et al. 2017). Notwithstanding, it deserves further investigation and is deferred for future work.

At multi-decadal or longer timescales, the study unveils an amplified sensitivity of the SAM, which is presumably attributed to coupled interactions. Two plausible reasons that support our inference are: firstly, the evolution of the SAM in the ESM and AMIP experiments is noticeably different where the feedback mechanisms are inherently absent on the latter, and, secondly, the fact that the SAM's vacillation has a similar trajectory in the AMIP, SSTclim and SICclim atmospheres rules out the assertion of individual merit. Notwithstanding, at the interannual or shorter timescales, the SAM trajectory is divergent and random. In addition,

although the SAM seems to be predictable at longer timescales, our result further strengthens the notion that the subseasonal to interannual predictability of the SAM is presumably unachievable even with the use of state-of-the-art ESMs. Other SH leading modes of climate variability are found to be increasingly sensitive to SST forcing at seasonal to longer timescales while the role of sea–ice forcing remains elusive.

Most of the changes on SH atmospheric circulation are explained by the SST forcing and coupled interactions. One probable justification is that the polar vortex signal is substantially reduced in the AMIP atmosphere relative to the ESM atmosphere. Although sea–ice forcing is found to play a role in modulating the atmospheric variability locally, it does not seem to perpetuate a hemispheric-wide atmospheric response. Nonetheless, it is unclear whether those changes on the atmospheric circulation, barely explained by the climate forcings considered here, are attributed to anthropogenic forcing or within the limits of intrinsic variability (such as multi-decadal or centennial). Generally, our findings support the notion that the underlying physical processes associated with the sea–ice variability and changes are presumably found mostly within the ocean thermal forcing. Last but not least, there may be room for uncertainty due to the fact that our sensitivity experiment is based on one model.

Acknowledgements

The authors are thankful to the Centre for High Performance Computing (CHPC) for providing computational facility. The work is supported by the National Research foundation (NRF, Grant No: 114689) through the Alliance for Collaboration on Climate & Earth Systems Science (ACCESS). We also acknowledge the iDEWS project, which supported the study under the auspices of the Japan Science and Technology Agency/Japan Agency for Medical Research and Development through the Science and Technology Research Partnership for Sustainable Development (SATREPS), and the ACCESS in South Africa. The authors also wish to thank the anonymous reviews for their valuable comments. Mostly, NCAR Command Language (NCL) was used for analysis and plotting (https://www.ncl.ucar.edu).

References

Ambrizzi T, Hoskins BJ, Hsu H-H (1995) Rossby wave propagation and teleconnection patterns in the austral winter. J Atmos Sci. https://doi.org/10.1175/1520-0469(1995)052%3c3661:RWPATP%3e2.0.CO;2

Arora VK, Harrison S (2007) Upscaling river networks for use in climate models. Geophys Res Lett. https://doi.org/10.1029/2007GL031865

Beraki AF, Dewitt DG, Landman WA, Olivier C (2014) Dynamical seasonal climate prediction using an ocean–atmosphere coupled climate model developed in partnership between South Africa and the IRI. J Clim. https://doi.org/10.1175/JCLI-D-13-00275.1

Berbery EH, Noguespaegle J, Horel JD (1992) Wave-like southern-hemisphere extratropical teleconnections. J Atmos Sci. https://doi.org/10.1175/1520-0469(1992)049%3c0155:WSHET%3e2.0.CO;2

Bi D, Budd WF, Hirst AC, Wu X (2001) Collapse and reorganisation of the Southern Ocean overturning under global warming in a coupled model. Geophys Res Lett. https://doi.org/10.1029/2001GL013705 Claussen M, Mysak L, Weaver A et al (2002) Earth system models of intermediate complexity: closing the gap in the spectrum of climate system models. Clim Dyn 18:579–586. https://doi.org/10.1007/s00382-001-0200-1

Colberg F, Reason CJC, Rodgers K (2004) South Atlantic response to El Niño-Southern Oscillation induced climate variability in an ocean general circulation model. J Geophys Res C Ocean. https://doi.org/10.1029/2004JC002301

Compo GP, Whitaker JS, Sardeshmukh PD (2008) The 20th century reanalysis project. In: Third WCRP international conference on reanalysis, The University of Tokyo, Japan. 28 Jan–1 Feb 2008

Compo GP, Whitaker JS, Sardeshmukh PD et al (2011) The twentieth century reanalysis project. Q J R Meteorol Soc. https://doi.org/10.1002/qj.776

Czaja A, Blunt N (2011) A new mechanism for ocean–atmosphere coupling in midlatitudes. Q J R Meteorol Soc. https://doi.org/10.1002/qj.814

Ding Q, Steig EJ, Battisti DS, Küttel M (2011) Winter warming in West Antarctica caused by central tropical Pacific warming. Nat Geosci. https://doi.org/10.1038/ngeo1129

Feng J, Li J, Li Y (2010) Is there a relationship between the SAM and Southwest Western Australian winter rainfall? J Clim. https://doi.org/10.1175/2010JCLI3667.1

Flato GM, Hibler WD (1992) Modeling pack ice as a cavitating fluid. J Phys Oceanogr. https://doi.org/10.1175/1520-0485(1992)022%3c0626:MPIAAC%3e2.0.CO;2

Fogt RL, Bromwich DH (2006) Decadal variability of the ENSO teleconnection to the high-latitude south pacific governed by coupling with the Southern Annular mode. J Clim. https://doi.org/10.1175/JCLI3671.1

Fogt RL, Wovrosh AJ (2015) The relative influence of tropical sea surface temperatures and radiative forcing on the Amundsen Sea Low. J Clim. https://doi.org/10.1175/JCLI-D-15-0091.1

Fogt RL, Zbacnik EA (2014) Sensitivity of the Amundsen sea low to stratospheric ozone depletion. J Clim. https://doi.org/10.1175/JCLI-D-13-00657.1

Folland C, Shukla J, Kinter J, Mark R (2002) The climate of the twentieth century project. CLIVAR Exch No 65, vol 19, no 2, pp 37–39

Gocic M, Trajkovic S (2013) Analysis of changes in meteorological variables using Mann–Kendall and Sen's slope estimator statistical tests in Serbia. Glob Planet Change. https://doi.org/10.1016/j.gloplacha.2012.10.014

Goosse H, Renssen H (2001) A two-phase response of the Southern Ocean to an increase in greenhouse gas concentrations. Geophys Res Lett. https://doi.org/10.1109/TBME.2016.2553177

Goosse H, Zunz V (2014) Decadal trends in the Antarctic sea ice extent ultimately controlled by ice–ocean feedback. Cryosphere. https://doi.org/10.5194/tc-8-453-2014

Gordon HB, O'Farrell SP (2002) Transient climate change in the CSIRO coupled model with dynamic sea ice. Mon Weather Rev. https://doi.org/10.1175/1520-0493(1997)125%3c0875:tccitc%3e2.0.co;2

Gordon HB, Rotstayn LD, McGregor JL, Dix MR, Kowalczyk EA, Ofarrell SP, Waterman LJ, Hirst AC, Wilson SG, Collier MA, Watterson IG, Elliott T (2002) The CSIRO Mk3 climate system model (electronic publication). Aspendale CSIRO Atmos Res (CSIRO Atmos Res Tech Pap no. 60). https://doi.org/10.4225/08/585974a670e09

Hall A, Visbeck M (2002) Synchronous variability in the Southern Hemisphere atmosphere, sea ice, and ocean resulting from the annular mode. J Clim. https://doi.org/10.1175/1520-0442(2002)015%3c3043:SVITSH%3e2.0.CO;2

Hamed KH, Ramachandra Rao A (1998) A modified Mann–Kendall trend test for autocorrelated data. J Hydrol. https://doi.org/10.1016/S0022-1694(97)00125-X

Hibler WD (1979) A dynamic thermodynamic sea ice model. J Phys Oceanogr. https://doi.org/10.1175/1520-0485(1979)009<0815:adtsim>2.0.co;2

Hobbs WR, Massom R, Stammerjohn S et al (2016) A review of recent changes in Southern Ocean sea ice, their drivers and forcings. Glob Planet Change 143:228–250. https://doi.org/10.1016/j.gloplacha.2016.06.008

Holland PR, Kwok R (2012) Wind-driven trends in Antarctic sea–ice drift. Nat Geosci. https://doi.org/10.1038/ngeo1627

Holland MM, Bitz CM, Hunke EC (2005) Mechanisms forcing an Antarctic dipole in simulated sea ice and surface ocean conditions. J Clim. https://doi.org/10.1175/JCLI3396.1

Holtslag AAM, Boville BA (1993) Local versus nonlocal boundary-layer diffusion in a global climate model. J Clim. https://doi.org/10.1175/1520-0442(1993)006%3c1825:LVNBLD%3e2.0.CO;2

Hosking JS, Orr A, Marshall GJ et al (2013) The influence of the Amundsen–Bellingshausen seas low on the climate of West Antarctica and its representation in coupled climate model simulations. J Clim. https://doi.org/10.1175/JCLI-D-12-00813.1

Hudson DA, Hewitson BC (2001) The atmospheric response to a reduction in summer Antarctic sea–ice extent. Clim Res. https://doi.org/10.3354/cr016079

Hunke EC, Dukowicz JK (2002) An elastic–viscous–plastic model for sea ice dynamics. J Phys Oceanogr. https://doi.org/10.1175/1520-0485(1997)027%3c1849:aevpmf%3e2.0.co;2

Jones DA, Simmonds I (1993) A climatology of Southern Hemisphere extratropical cyclones. Clim Dyn. https://doi.org/10.1007/BF00209750

Jones JM, Gille ST, Goosse H et al (2016) Assessing recent trends in high-latitude Southern Hemisphere surface climate. Nat Clim Chang 6:917–926. https://doi.org/10.1038/nclimate3103

Kanamitsu M, Ebisuzaki W, Woollen J et al (2002) NCEP-DOE AMIP-II reanalysis (R-2). Bull Am Meteorol Soc. https://doi.org/10.1175/BAMS-83-11-1631(2002)083%3c1631:NAR%3e2.3.CO;2

Karoly DJ (1989) Southern hemisphere circulation features associated with El Niño-Southern oscillation events. J Clim. https://doi.org/10.1175/1520-0442(1989)002%3c1239:SHCFAW%3e2.0.CO;2

Kidston J, Renwick JA, McGregor J (2009) Hemispheric-scale seasonality of the southern annular mode and impacts on the climate of New Zealand. J Clim. https://doi.org/10.1175/2009JCLI2640.1

Kowalczyk E, Stevens L, Law R et al (2013) The land surface model component of ACCESS: description and impact on the simulated surface climatology. Aust Meteorol Oceanogr J. https://doi.org/10.22499/2.6301.005

Kreyscher M, Harder M, Lemke P, Flato GM (2002) Results of the sea ice model intercomparison project: evaluation of sea ice rheology schemes for use in climate simulations. J Geophys Res Ocean. https://doi.org/10.1029/1999jc000016

Lefebvre W, Goosse H, Timmermann R, Fichefet T (2004) Influence of the Southern Annular Mode on the sea ice—ocean system. J Geophys Res C Ocean. https://doi.org/10.1029/2004JC002403

Lemke P, Trinkl EW, Hasselmann K (1980) Stochastic dynamic analysis of polar sea ice variability. J Phys Ocean. https://doi.org/10.1175/1520-0485(1980)010%3c2100:SDAOPS%3e2.0.CO;2

Li X, Holland DM, Gerber EP, Yoo C (2014) Impacts of the north and tropical Atlantic Ocean on the Antarctic Peninsula and sea ice. Nature. https://doi.org/10.1038/nature12945

Limpasuvan V, Hartmann DL (2000) Wave-maintained annular modes of climate variability. J Clim. https://doi.org/10.1175/1520-0442(2000)013%3c4414:WMAMOC%3e2.0.CO;2

Liu J, Curry JA (2010) Accelerated warming of the Southern Ocean and its impacts on the hydrological cycle and sea ice. Proc Natl Acad Sci. https://doi.org/10.1073/pnas.1003336107

Mahlstein I, Gent PR, Solomon S (2013) Historical Antarctic mean sea ice area, sea ice trends, and winds in CMIP5 simulations. J Geophys Res Atmos. https://doi.org/10.1002/jgrd.50443

Marshall GJ (2003) Trends in the Southern Annular Mode from observations and reanalyses. J Clim. https://doi.org/10.1175/1520-0442(2003)016%3c4134:TITSAM%3e2.0.CO;2

McGregor JL (2003) A new convection scheme using a simple closure. In “Current issues in the parameterization of convection”. BMRC Res Report 93:33–36

McGregor JL (2005) Geostrophic adjustment for reversibly staggered grids. Mon Weather Rev. https://doi.org/10.1175/MWR2908.1

McGregor JL, Dix MR (2008) An updated description of the conformal-cubic atmospheric model. In: High resolution numerical modelling of the atmosphere and ocean. Springer; New York, London, pp 52–75. http://hdl.handle.net/102.100.100/118189?index=1

Mestas-Nuñez AM (2000) Orthogonality properties of rotated empirical modes. Int J Climatol. https://doi.org/10.1002/1097-0088(200010)20:12%3c1509:AID-JOC553%3e3.0.CO;2-Q

Minobe S, Kuwano-Yoshida A, Komori N et al (2008) Influence of the Gulf Stream on the troposphere. Nature. https://doi.org/10.1038/nature06690

Mitchell JFB, Senior CA (1989) The antarctic winter; simulations with climatological and reduced sea–ice extents. Q J R Meteorol Soc. https://doi.org/10.1002/qj.49711548602

Mitchell JFB, Davis RA, Ingram WJ, Senior CA (1995) On surface temperature, greenhouse gases, and aerosols: models and observations. J Clim. https://doi.org/10.1175/1520-0442(1995)008%3c2364:OSTGGA%3e2.0.CO;2

Mo KC, Higgins RW (1998) The Pacific-South American Modes and Tropical Convection during the Southern Hemisphere Winter. Mon Weather Rev. https://doi.org/10.1175/1520-0493(1998)126%3c1581:TPSAMA%3e2.0.CO;2

Morioka Y, Ratnam JV, Sasaki W, Masumoto Y (2013) Generation mechanism of the South Pacific subtropical dipole. J Clim. https://doi.org/10.1175/JCLI-D-12-00648.1

Morioka Y, Engelbrecht F, Behera SK (2017) Role of Weddell Sea ice in South Atlantic atmospheric variability. Clim Res. https://doi.org/10.3354/cr01495

Murphy AH (1988) Skill scores based on the mean square error and their relationships to the correlation coefficient. Mon Weather Rev. https://doi.org/10.1175/1520-0493(1988)116%3c2417:SSBOTM%3e2.0.CO;2

North GR, Bell TL, Cahalan RF, Moeng FJ (1982) Sampling errors in the estimation of empirical orthogonal functions. Mon Weather Rev. https://doi.org/10.1175/1520-0493(1982)110%3c0699:seiteo%3e2.0.co;2

O'Farrell SP (2004) Investigation of the dynamic sea ice component of a coupled atmosphere–sea ice general circulation model. J Geophys Res Ocean. https://doi.org/10.1029/98jc00815

Pepler A, Dowdy A, Hope P (2018) A global climatology of surface anticyclones, their variability, associated drivers and long-term trends. Clim Dyn 52:5397–5412. https://doi.org/10.1007/s00382-018-4451-5

Pezza AB, Rashid HA, Simmonds I (2012) Climate links and recent extremes in antarctic sea ice, high-latitude cyclones Southern Annular Mode and ENSO. Clim Dyn. https://doi.org/10.1007/s00382-011-1044-y

Purich A, Cai W, England MH, Cowan T (2016) Evidence for link between modelled trends in Antarctic sea ice and underestimated westerly wind changes. Nat Commun. https://doi.org/10.1038/ncomms10409

Raphael MN (2003) Impact of observed sea–ice concentration on the Southern Hemisphere extratropical atmospheric circulation in summer. J Geophys Res. https://doi.org/10.1029/2002JD003308

Raphael MN (2007) The influence of atmospheric zonal wave three on Antarctic sea ice variability. J Geophys Res Atmos. https://doi.org/10.1029/2006JD007852

Rayner NA, Parker DE, Horton EB et al (2003) Globally complete analyses of sea surface temperature, sea ice and night marine air temperature, 1871–2000. J Geophys Res. https://doi.org/10.1029/2002JD002670

Reason CJC, Rouault M (2005) Links between the Antarctic Oscillation and winter rainfall over western South Africa. Geophys Res Lett. https://doi.org/10.1029/2005GL022419

Rotstayn LD (1997) A physically based scheme for the treatment of stratiform clouds and precipitation in large-scale models. I: Description and evaluation of the microphysical processes. Q J R Meteorol Soc. https://doi.org/10.1002/qj.49712354106

Rousset C, Vancoppenolle M, Madec G et al (2015) The Louvain-La-Neuve sea ice model LIM3.6: global and regional capabilities. Geosci Model Dev. https://doi.org/10.5194/gmd-8-2991-2015

Schneider DP, Okumura Y, Deser C (2012) Observed Antarctic interannual climate variability and tropical linkages. J Clim. https://doi.org/10.1175/JCLI-D-11-00273.1

Schulkes RMSM, Morland LW, Staroszczyk R (1998) A finite-element treatment of sea ice dynamics for different ice rheologies. Int J Numer Anal Methods Geomech. https://doi.org/10.1002/(SICI)1096-9853(199803)22:3%3c153:AID-NAG912%3e3.0.CO;2-E

Sen GA, England MH (2006) Coupled ocean–atmosphere–ice response to variations in the southern annular mode. J Clim. https://doi.org/10.1175/JCLI3843.1

Silvestri GE, Vera CS (2003) Antarctic Oscillation signal on precipitation anomalies over southeastern South America. Geophys Res Lett. https://doi.org/10.1029/2003GL018277

Simmonds I, Wu X (1993) Cyclone behaviour response to changes in winter southern hemisphere sea–ice concentration. Q J R Meteorol Soc. https://doi.org/10.1002/qj.49711951313

Simpkins GR, Ciasto LM, Thompson DWJ, England MH (2012) Seasonal relationships between large-scale climate variability and antarctic sea ice concentration. J Clim. https://doi.org/10.1175/JCLI-D-11-00367.1

Stammerjohn SE, Martinson DG, Smith RC et al (2008) Trends in Antarctic annual sea ice retreat and advance and their relation to El Niño-Southern Oscillation and Southern Annular Mode variability. J Geophys Res. https://doi.org/10.1029/2007JC004269

Stouffer RJ, Manabe S, Bryan K (1989) Interhemispheric asymmetry in climate response to a gradual increase of atmospheric CO_2. Nature. https://doi.org/10.1038/342660a0

Swart NC, Fyfe JC (2013) The influence of recent Antarctic ice sheet retreat on simulated sea ice area trends. Geophys Res Lett. https://doi.org/10.1002/grl.50820

Taylor KE (2001) Summarizing multiple aspects of model performance in a single diagram. J Geophys Res Atmos. https://doi.org/10.1029/2000JD900719

Taylor KE, Stouffer RJ, Meehl GA (2012) An overview of CMIP5 and experimental design. Bull Am Meteorol Soc. https://doi.org/10.1175/BAMS-D-11-00094.1

Thatcher M, McGregor JL (2011) A technique for dynamically downscaling daily-averaged GCM datasets using the conformal cubic atmospheric model. Mon Weather Rev. https://doi.org/10.1175/2010MWR3351.1

Thatcher M, McGregor J, Dix M, Katzfey J (2015) A New approach for coupled regional climate modeling using more than 10,000 cores. In: Denzer R, Argent RM, Schimak GHJ (eds) Environmental software systems. Infrastructures, services and applications. ISESS 2015. IFIP advances in information and communication technology, vol 448. Springer, Cham

Thompson DWJ, Wallace JM (2000) Annular modes in the extratropical circulation. Part I: Month-to-month variability. J Clim. https://doi.org/10.1175/1520-0442(2000)013%3c1000:AMITEC%3e2.0.CO;2

Trenberth KE, Fasullo JT, Branstator G, Phillips AS (2014) Seasonal aspects of the recent pause in surface warming. Nat Clim Change. https://doi.org/10.1038/nclimate2341

Turner J (2004) The El Niño-Southern Oscillation and Antarctica. Int J Climatol. https://doi.org/10.1002/joc.965

Turney CSM, McGlone M, Palmer J et al (2016) Intensification of Southern Hemisphere westerly winds 2000–1000 years ago: evidence from the subantarctic Campbell and Auckland Islands (52°–50° S). J Quat Sci. https://doi.org/10.1002/jqs.2828

Turney CSM, Fogwill CJ, Palmer JG et al (2017) Tropical forcing of increased Southern Ocean climate variability revealed by a 140-year subantarctic temperature reconstruction. Clim Past. https://doi.org/10.5194/cp-13-231-2017

Van Den Broeke M (2000) The semi-annual oscillation and Antarctic climate. Part 4: A note on sea ice cover in the Amundsen and Bellingshausen Seas. Int J Climatol. https://doi.org/10.1002/(SICI)1097-0088(20000330)20:4%3c455:AID-JOC482%3e3.0.CO;2-M

Wallace JM, Hsu H-H (1983) Ultra-long waves and two-dimensional Rossby waves. J Atmos Sci 40:2211–2219

Wang G, Dommenget D (2016) The leading modes of decadal SST variability in the Southern Ocean in CMIP5 simulations. Clim Dyn. https://doi.org/10.1007/s00382-015-2932-3

Wang G, Dommenget D, Frauen C (2014) An evaluation of the CMIP3 and CMIP5 simulations in their skill of simulating the spatial structure of SST variability. Clim Dyn. https://doi.org/10.1007/s00382-014-2154-0

Waugh DW, Sobel AH, Polvani LM (2017) What is the polar vortex and how does it influence weather? Bull Am Meteorol Soc. https://doi.org/10.1175/BAMS-D-15-00212.1

White WB, Simmonds I (2006) Sea surface temperature-induced cyclogenesis in the Antarctic circumpolar wave. J Geophys Res Ocean. https://doi.org/10.1029/2004JC002395

Wu Z, Huang NE, Long SR, Peng C-K (2007) On the trend, detrending, and variability of nonlinear and nonstationary time series. Proc Natl Acad Sci. https://doi.org/10.1073/pnas.0701020104

Xu S, Song M, Liu J et al (2013) Simulation of sea ice in FGOALS-g2: climatology and late 20th century changes. Adv Atmos Sci. https://doi.org/10.1007/s00376-013-2158-4

Yuan X (2004) ENSO-related impacts on Antarctic sea ice: a synthesis of phenomenon and mechanisms. Antarct Sci. https://doi.org/10.1017/S0954102004002238 Yuan X, Li C (2008) Climate modes in southern high latitudes and their impacts on Antarctic sea ice. J Geophys Res Ocean. https://doi.org/10.1029/2006JC004067

Yuan X, Martinson DG (2001) The Antarctic dipole and its predictability. Geophys Res Lett. https://doi.org/10.1029/2001GL012969